Book Section:
Bhowmik, D. and Abhayaratne, C. (2009) A generalised model for distortion performance analysis of wavelet based watermarking. In: Kim, H.J., Katzenbeisser, S. and Ho, A. T. S. , (eds.) Digital Watermarking. Springer Berlin Heidelberg, pp. 363-378. ISSN: 0302-9743.

https://doi.org/10.1007/978-3-642-04438-0_31

A Generalised Model for Distortion Performance Analysis of Wavelet based Watermarking

Deepayan Bhowmik and Charith Abhayaratne

Department of Electronic and Electrical Engineering, University of Sheffield
Sheffield S1 3JD, United Kingdom.
{d.bhowmik, c.abhayaratne}@sheffield.ac.uk

Abstract. A model for embedding distortion performance for wavelet based watermarking is presented in this paper. Firstly wavelet based watermarking schemes are generalised into a single common framework. Then a mathematical approach has been made to find the relationship between distortion performance metrics and the watermark embedding parameters. The derived model shows that for wavelet based watermarking schemes the sum of energy of the selected wavelet coefficients to be modified is directly proportional to the distortion performance (the mean square error) measured in the pixel domain. The propositions are made using the energy conservation theorem between input signal and transform domain coefficients for orthonormal wavelet bases. Such an analysis is useful to choose the wavelet coefficients during watermark embedding procedure and to find suitable input parameters such as wavelet kernel or the choice of subband.

Key words: Watermarking, wavelet transforms, distortion performance.

1 Introduction

With the success of transforms based image/video compression schemes, such as, JPEG, JPEG2000 and MPEG-2, the frequency domain watermarking has received a huge attention. The discrete wavelet transform (DWT) has been widely used as a multi-resolution analysis method in most frequency domain watermarking techniques. [1–11]. Usually the imperceptibility and robustness are considered as two major properties of any watermarking scheme. The imperceptibility is often measured by evaluating the distortion of the host image.

In this work we address the problem of modelling and analysis of embedding distortion. In the literature, such analysis have been presented by only focusing on single specific techniques [12]. Our focus in this paper is to derive a common analysis model involving an exhaustive list of wavelet based algorithms characterised by their input parameters. The main objective of the work is to derive a generalised model for distortion performance analysis of wavelet based watermarking. The generalisation of our model is based on fitting all major wavelet based watermarking schemes into a common framework, which was presented in [13].

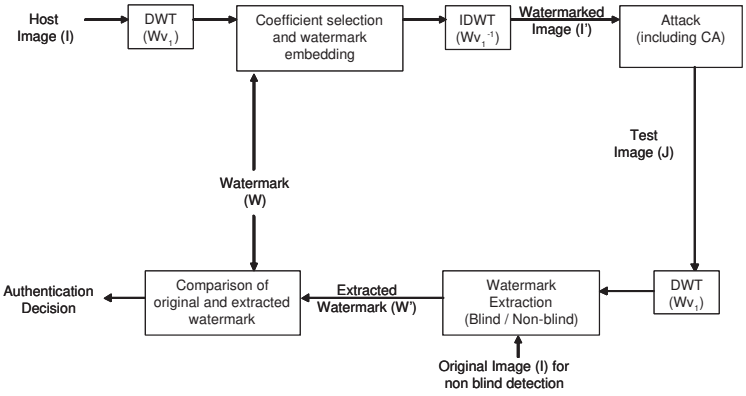

Fig. 1. Block diagram of the generalised functional modules of wavelet based watermarking schemes.

In the distortion performance model first a proposition is made to show the relationship between the noise power in the transform domain and the input signal domain. Then using the above proposition a relationship is established between the distortion performance metrics and the input parameters of a given wavelet based watermarking scheme. The rest of the paper is organised with Sect. 2 presenting the generalisation of embedding schemes. Detailed mathematical analysis and the model is presented in Sect. 3 followed by experimental results in Sect. 4. Concluding remarks can be found in Sect. 5.

2 The common framework for wavelet based watermark embedding

There are many wavelet based watermarking schemes available in the literature. In this context a formal evaluation framework for wavelet based methods is really useful to the watermarking community. It is observed that most of the popular wavelet based watermarking schemes can be dissected in common functional blocks as shown in Fig. 1. In this paper we discuss and present the distortion performance model of wavelet based algorithms and therefore restrict our discussion to the embedding part of the watermarking schemes. In a more general form of the watermarking schemes a forward wavelet transform is applied to the target image. The wavelet coefficients are then modified according to the particular embedding procedure. The modification is done on the selected coefficients in the selected subbands. An inverse wavelet transform which is the same as the forward wavelet kernel is then applied to produce the watermarked image. The basic embedding principle for any wavelet based watermarking algorithm is the same and the modified coefficient $C'_{m,n}$ at (m, n) position, can be presented as:

$$C'_{m,n} = C_{m,n} + \Delta_{m,n} \ , \tag{1}$$

Table 1. Realisation of wavelet based algorithms using different combination of input parameters

Method	Selection Coeff $< a_1, a_2, a_3, a_4 >$	Subband Selection	Wavelet Kernel	Level	Reference	Δ as Function of
Direct($b = 2$)	$< 1, 0, 0, 0 >$	High	Haar	2	[1]	$f(C_{m,n})$
Direct($b = 1$)	$< 1, 0, 0, 0 >$	All	Biorthogonal	3	[2]	$f(C_{m,n})$
Direct($b = 1$)	$< 1, 0, 0, 0 >$	Low	Biorthogonal, Non-linear	3	[14]	$f(C_{m,n})$
Direct	$< 0, 0, 1, 0 >$	High	Orthogonal	4	[11]	$f(C_{m,n})$
Direct	$< 0, 0, 0, 1 >$	High	Any	2	[10]	$f(C_{m,n})$
Quantisation	-	Low	Any	2	[6]	$f(C_{min}, C_{max})$
Quantisation	-	High	Haar	1	[4]	$f(C_{min}, C_{max})$
Quantisation	-	High	Any	2	[3]	$f(C_{min}, C_{max})$

where $C_{m,n}$ is the coefficient to be modified and $\Delta_{m,n}$ is the modification due to watermark embedding. Based on the modification algorithms, the embedding procedures are categorised into two main types of embedding algorithms: direct coefficient modification [1, 2, 7, 10, 11] and quantisation based modification [4, 6, 8, 3].

In the direct coefficient modification schemes, selected coefficients are directly modified based on the following generalised modification value $\Delta_{m,n}$ at (m, n) position:

$$\Delta_{m,n} = (a_1)\alpha(C_{m,n})^b W_{m,n} + (a_2)v_{m,n}W_{m,n} + (a_3)\beta C_w + (a_4)S_{m,n} \ , \qquad (2)$$

where a_1, a_2, a_3, a_4 are the selection coefficients, $C_{m,n}$ is the coefficient to be modified, α is the watermark weighting factor, $b = 1, 2...$ is the watermark strength parameter, $W_{m,n}$ is the watermark value, $v_{m,n}$ is the weighting parameter based on pixel masking in HVS model, β is the weighting parameter in the case of fusion based scheme, C_w is the watermark wavelet coefficient and $S_{m,n}$ is any other value which is normally a function of $C_{m,n}$. In most of the algorithms watermark weighting parameters α and β are user defined to an optimal value. The watermark information $W_{m,n}$ is either generated randomly with a random seed or taken from a gray scale logo or a binary logo. As mentioned before the weighting parameter and the watermark information are always user defined, hence these are considered as constant parameters in a controlled experimental environment. Other parameters in the modification equation are a function of the wavelet coefficient $C_{m,n}$ which depends on the input image and considered as a variable here. Therefore it is observed that in all the cases the modification value is a direct function of the coefficient $C_{m,n}$ as mentioned in Table 1. This table also represents the common input parameters used in the embedding procedure and shows how different algorithms can be realised with this generalised framework. Considering a specific case, in this paper we have not chosen HVS model based watermarking scheme as our main focus is on distortion performance analysis which is different from HVS based performance metrics.

On the other hand in the case of quantisation based algorithms, the modification is based on the quantisation steps. Normally a rank order based algorithm

is proposed in these type algorithms. The algorithms change the median value of a local area (typically a 3x1 coefficient window) considering the neighbouring values. The modification value $\Delta_{m,n}$ is decided based on the quantisation step δ ($-\delta \leq \Delta \leq \delta$) within the range of the selected 3x1 window. Different functions are suggested in the literature to find the value of δ and the functions normally consist of minimum (C_{min}) and maximum (C_{max}) value of the coefficients in each selected window. A predefined weighting factor α is often used to determine the value of δ. As Δ depends on step size δ and α is user defined, the modification value Δ is typically a function of C_{min} and C_{max} in each selected 3x1 window (refer Table 1).

With this common generalised framework we have analysed and proposed a distortion performance model in the next section.

3 Embedding Distortion Performance Analysis

In this section a detailed discussion is carried out on the proposed model. The embedding distortion performance is usually measured by the Mean Square Error (MSE).

Definition 1. The *Mean Square Error (MSE)* or average noise power P_p in pixel domain between original image I and watermarked image I' is defined by:

$$P_p = \frac{1}{MN} \sum_{j=0}^{M-1} \sum_{i=0}^{N-1} |I(j,i) - I'(j,i)|^2 \ , \tag{3}$$

where M and N are the image dimension and j and i indicate each pixel position.

In order to formulate the model we show the transformation of noise energy from frequency domain to the signal domain using Parseval's equality.

Definition 2. In the *Parseval's Equality*, the energy is conserved between an input signal and the transform domain coefficient in the case of an orthonormal filter bank wavelet base [15]. Assuming the input signal $x[n]$ with the length of $n \in Z$ and the corresponding transformed domain coefficients of $y[k]$ where $k \in Z$, according to energy conservation theorem,

$$\|x\|^2 = \|y\|^2 \ . \tag{4}$$

Based on these primary definitions we build the model which consists of the following propositions and its proof.

Proposition 1. *Sum of the noise power in the transform domain is equal to sum of the noise power in the input signal for orthonormal transforms. If the input signal noise is defined by $\Delta x[n]$ and the noise in transform domain is $\Delta y[k]$ then*

$$\sum_n |\Delta x[n]|^2 = \sum_k |\Delta y[k]|^2 \ , \tag{5}$$

where $n \in Z$ is the length of the input signal and $k \in Z$ is the length in the transform domain, respectively.

Proof. The discrete wavelet transform (DWT) can be realised with a filter bank or lifting scheme based factoring. In both cases the wavelet decomposition and the reconstruction can be represented by a polyphase matrix [16]. The inverse DWT can be defined by a synthesis filter bank using the polyphase matrix $M'(z) = \begin{pmatrix} h'_e(z) & h'_o(z) \\ g'_e(z) & g'_o(z) \end{pmatrix}$ where $h'(z)$ represents the low pass filter coefficients and $g'(z)$ is the high pass filter coefficients and the subscripts e and o denote even and odd indexed terms, respectively. Now the transform domain coefficient y can be re-mapped into input signal x as bellow:

$$\begin{pmatrix} x_e(z) \\ x_o(z) \end{pmatrix} = \begin{pmatrix} h'_e(z) & h'_o(z) \\ g'_e(z) & g'_o(z) \end{pmatrix} \begin{pmatrix} y_e(z) \\ y_o(z) \end{pmatrix} . \tag{6}$$

Assuming Δy is the noise introduced in wavelet domain and Δx is the modified signal after the inverse transform, we can define the relationship between the noise in the wavelet coefficient and the noise in the modified signal using the following equations. From (6) we can write

$$\begin{pmatrix} x_e(z)+\Delta x_e(z) \\ x_o(z)+\Delta x_o(z) \end{pmatrix} = \begin{pmatrix} h'_e(z) & h'_o(z) \\ g'_e(z) & g'_o(z) \end{pmatrix} \begin{pmatrix} y_e(z)+\Delta y_e(z) \\ y_o(z)+\Delta y_o(z) \end{pmatrix} . \tag{7}$$

From (7) using the *Linearity* property of the Z transform of the filter coefficients and signals in the polyphase matrix we can get,

$$\begin{aligned} x_e(z) + \Delta x_e(z) &= h'_e(z)(y_e(z) + \Delta y_e(z)) \\ &\quad + h'_o(z)(y_o(z) + \Delta y_o(z)) , \\ h'_e(z)y_e(z) + h'_o(z)y_o(z) + \Delta x_e(z) &= h'_e(z)y_e(z) + h'_e(z)\Delta y_e(z) \\ &\quad + h'_o(z)y_o(z) + h'_o(z)\Delta y_o(z) , \\ \Delta x_e(z) &= h'_e(z)\Delta y_e(z) + h'_o(z)\Delta y_o(z) . \end{aligned} \tag{8}$$

Similarly $\Delta x_o(z)$ can be obtained and written as

$$\Delta x_o(z) = g'_e(z)\Delta y_e(z) + g'_o(z)\Delta y_o(z) . \tag{9}$$

Combining (8) and (9), finally we can write the polyphase matrix form of the noise in the output signal:

$$\begin{pmatrix} \Delta x_e(z) \\ \Delta x_o(z) \end{pmatrix} = \begin{pmatrix} h'_e(z) & h'_o(z) \\ g'_e(z) & g'_o(z) \end{pmatrix} \begin{pmatrix} \Delta y_e(z) \\ \Delta y_o(z) \end{pmatrix} . \tag{10}$$

Recalling the Parseval's energy conservation theorem as stated in *Definition 2.*, from (10) we can conclude that

$$\begin{aligned} \sum |\Delta x_e|^2 + \sum |\Delta x_o|^2 &= \sum |\Delta y_e|^2 + \sum |\Delta y_o|^2 , \\ \sum_n |\Delta x[n]|^2 &= \sum_k |\Delta y[k]|^2 . \end{aligned} \tag{11}$$

■

Using the generalised framework, the *Proposition 1* can be applied to build the relationship between the modification energy in the coefficient domain to embed the watermark and the distortion performance metrics. In this model we made propositions for two different categories of embedding schemes, discussed in previous section.

Proposition 2. *In a wavelet based watermarking scheme, the mean square error (MSE) of the watermarked image is directly proportional to the sum of the energy of the modification values of the selected wavelet coefficients. The modification value itself is a function of the wavelet coefficients and therefore we propose two different cases based on the categorisation.*

Case A. *For the direct modification embedding method the modification is a function of the selected coefficient to be watermarked and the relationship between MSE (P_p) and the selected coefficient ($C_{m,n}$) is expressed as:*

$$P_p \propto \sum |f(C_{m,n})|^2 \ . \tag{12}$$

Case B. *For the quantisation based method the modification is a function of the neighbouring wavelet coefficients of the selected median coefficient to be watermarked and the relationship between MSE (P_p) and the wavelet coefficients C_{min} and C_{max} is expressed as:*

$$P_p \propto \sum |f(C_{min}, C_{max})|^2 \ . \tag{13}$$

Proof. In a wavelet based watermark embedding scheme the watermark information is inserted by modifying the wavelet coefficients. This watermark insertion can be considered as introducing noise in the transform domain. Hence the sum of the energy of the modification value due to watermark embedding in the wavelet domain is equal to the sum of the noise energy in the transform domain as stated in *Proposition 1.* From (1) and (5), the energy sum of the modification value $\Delta_{m,n}$ can be defined as:

$$\sum_{m,n} |\Delta_{m,n}|^2 = \sum_{k} |\Delta y[k]|^2 \ . \tag{14}$$

Similarly, the pixel domain distortion performance metrics which is represented by MSE is considered as the noise error created in the signal due to the noise in wavelet domain. Therefore, the sum of the noise energy in the input signal is equal to the sum of the noise error energy P_p in the pixel domain:

$$P_p.(MN) = \sum_{n} |\Delta x[n]|^2 \ , \tag{15}$$

where M and N are the image dimensions. Now the relationship between the distortion performance metrics MSE of the watermarked image and the coefficient modification value which is normally a function of the selected wavelet coefficients can be decided using the *Proposition 1.* Thus from (14) and (15) we can write:

$$P_p.(MN) = \textstyle\sum_{m,n} |\Delta_{m,n}|^2 \ , \tag{16}$$

where M and N are the image dimensions. Hence for any watermarked image, the average noise power P_p is proportional to the sum of the energy of the modification values of the selected wavelet coefficients:

$$P_p \propto \sum_{m,n} |\Delta_{m,n}|^2 \ . \tag{17}$$

Now with the help of the categorisation in the generalised form of the popular wavelet based watermarking schemes as discussed in Sect. 2, a relationship is established between the error energy of the watermarked image and the selected wavelet coefficient energy of the host image. For a direct modification based algorithm, the mean square error P_p is directly proportional to the sum of the energy of the modification value Δ which is a function of wavelet coefficient value as stated below:

$$P_p \propto \sum |f(C_{m,n})|^2 \ . \tag{18}$$

Similarly for the quantisation based method the mean square error depends on the neighbouring wavelet coefficient values. In this case the modification energy $|\Delta_{m,n}|^2$ hold an inequality due the modification range $-\delta \leq \Delta_{m,n} \leq \delta$:

$$|\Delta_{m,n}|^2 \leq |\delta|^2 \ . \tag{19}$$

Therefore the upper bound of the mean square error P_p is defined by:

$$P_p \propto \sum |f(C_{min}, C_{max})|^2 \ . \tag{20}$$

■

3.1 An Example of Direct Modification

Considering a specific case of the direct modification algorithm in [2] the modification value Δ is a direct function of wavelet coefficient ($\Delta_{m,n} = \alpha C_{m,n} W m, n$). Hence (18) can be modified and the MSE P_p can be expressed as:

$$P_p \propto \sum_{k=1}^{l} |C(k)|^2 \ , \tag{21}$$

where $C(k)$ is the selected coefficients to be watermarked and l is the number of such selected coefficients.

3.2 An Example of Quantisation based Method

In an intra subband based quantisation method suggested in [6], the quantisation step δ is defined as:

$$\delta = \alpha \frac{C_{max} + C_{min}}{2} \ , \tag{22}$$

where α is the user defined weighting factor. As the modification value Δ depends on δ, with reference to (20), the relationship between the maximum limit of MSE P_p and wavelet energy is defined by the following equation:

$$P_p \propto \sum_{k} (C(k)_{max} + C(k)_{min})^2 \ , \tag{23}$$

where $C(k)_{max}$ and $C(k)_{min}$ are the neighbourhood coefficients of the median value and l is the number of such selected median value.

Table 2. Correlation coefficient values between sum of energy and the MSE for different wavelet kernel in various subbands.

	Direct modification						Intra Subband Based					
	Haar	D-4	D-6	D-8	D-10	D-16	Haar	D-4	D-6	D-8	D-10	D-16
LL3	0.99	0.99	0.99	0.99	0.99	0.99	0.80	0.84	0.87	0.88	0.86	0.89
LH3	0.99	0.99	0.99	0.99	0.99	0.99	0.99	0.99	0.99	0.99	0.99	0.99
HL3	0.99	0.99	0.99	0.99	0.99	0.99	0.93	0.96	0.95	0.96	0.97	0.99
HH3	0.99	0.99	0.99	0.99	0.99	0.99	0.99	0.99	0.99	0.99	0.99	0.99
LH2	0.99	0.99	0.99	0.99	0.99	0.99	0.99	0.99	0.99	0.99	0.99	0.99
HL2	0.99	0.99	0.99	0.99	0.99	0.99	0.99	0.99	0.99	0.99	0.99	0.99
HH2	0.99	0.99	0.99	0.99	0.99	0.99	0.99	0.99	0.99	0.99	0.99	0.99
LH1	0.99	0.99	0.99	0.99	0.99	0.99	0.99	0.99	0.99	0.99	0.99	0.99
HL1	0.99	0.99	0.99	0.99	0.99	0.99	0.97	0.98	0.99	0.98	0.98	0.99
HH1	0.99	0.99	0.99	0.99	0.99	0.99	0.99	0.99	0.99	0.99	0.99	0.99

4 Experimental Simulations

The propositions made in the previous section are verified in the experimental simulations. The sum of the energy of the selected wavelet coefficients and the MSE of the watermarked image have been calculated for 30 different images with a combination of different input parameters. As the wavelet coefficients varies greatly in different subbands we have considered the performances of all subbands separately after a 3 level wavelet decomposition. Also a set of different wavelet kernels having various filter lengths are selected to perform the simulations. We simulated and studied the performance of different wavelet kernels such as Haar, Daubechies-4 (D-4), Daubechies-6 (D-6), Daubechies-8 (D-8), Daubechies-10 (D-10) and Daubechies-16 (D-16) in order to verify our proposed model. Two different sets of results are obtained and displayed to verify the effects of different input parameters which are responsible for embedding distortion performance. These two sets of experimental arrangements and resulting plots are discussed separately as follows:

- In the experiment *Set 1*, the sum of energy of the selected wavelet coefficients to be modified and MSE of the watermarked image have been calculated using the same α and the same binary watermark logo for each selected method. We have used various wavelet kernels and observed the results for each selected subbands. The correlation between MSE and the energy sum is displayed in Fig. 2 and Fig. 3 for direct modification and intra subband based embedding, respectively. The correlation coefficients are also calculated and presented in Table 2.
  In another representation a set of graphs are plotted in Fig. 4 and Fig. 5 for direct modification and in Fig. 6 for intra subband based embedding. These plots present the average values of the MSE and the sum of energy for the test image set. The error bars denote the accuracy up to the 95% confidence interval. For display purposes the sum of energy value was scaled, so that they can be shown on the same plot for comparing the trend.

– In the experiment *Set 2*, the performance for different subbands are plotted for each wavelet kernel in a similar fashion as mentioned in experiment *Set 1* in order to observe the trend. The direct modification results are shown in Fig. 7 and the intra subband modification methods are shown in Fig. 8. As earlier, a 95% confidence interval is considered which is denoted by the error bars.

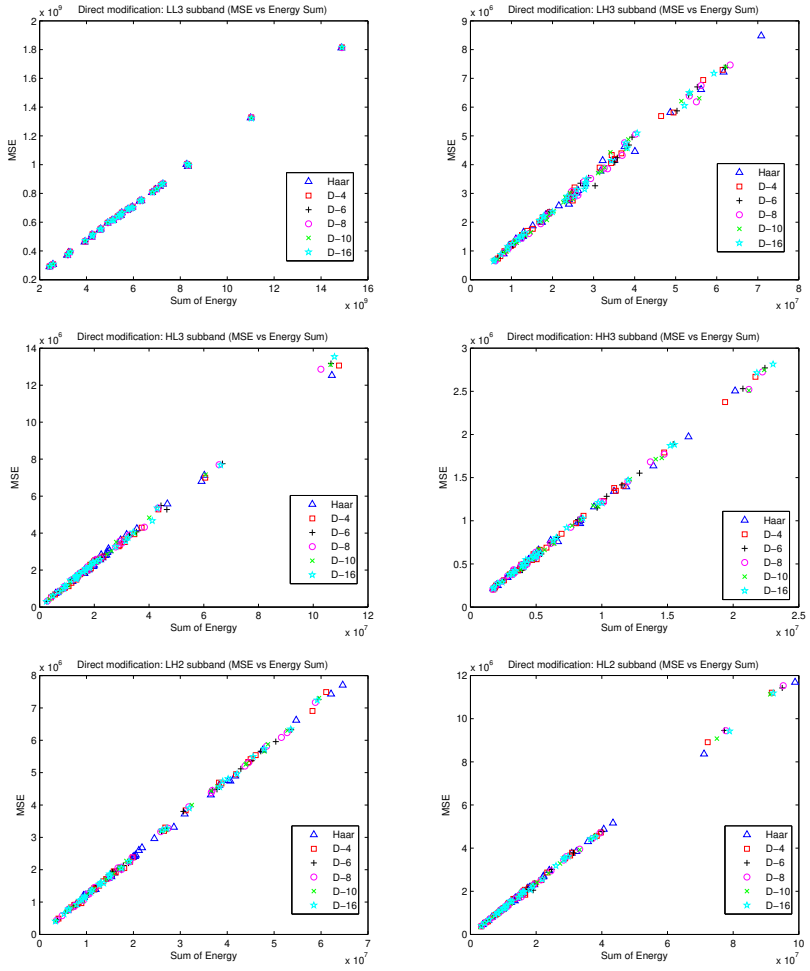

Fig. 2. Watermark embedding (Direct Modification) performance correlation plot: MSE vs. sum of energy, in different subband for individual images. Six wavelet kernels used here such as 1. Haar, 2. D-4, 3. D-6, 4. D-8, 5. D-10 and 6. D-16, respectively.

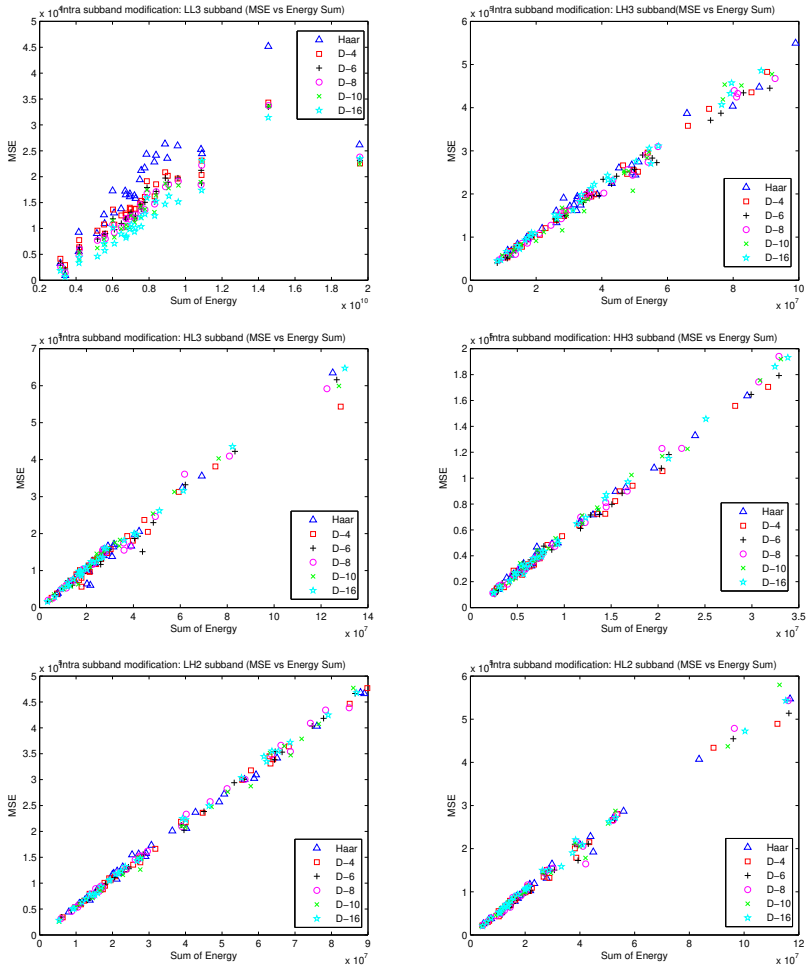

Fig. 3. Watermark embedding (Intra subband based) performance correlation plot: MSE vs. sum of energy, in different subband for individual images. Six wavelet kernels used here such as 1. Haar, 2. D-4, 3. D-6, 4. D-8, 5. D-10 and 6. D-16, respectively.

The simulation results show a strong correlation between MSE of the watermarked image and the energy sum of the selected wavelet coefficients to be modified. It is observed that for a direct modification, the correlation coefficient value is more than 0.97 and more than 0.80 in the case of intra subband based modification, for different wavelet kernels and various selected subbands. On the other hand, a similar graph patterns are observed in Fig. 4, Fig. 5, Fig. 6, Fig. 7 and Fig. 8, which show the proportionality trend between MSE and the energy sum as proposed in the model.

These extensive simulation results strongly support the proposed model for a wide range of input images and various orthogonal wavelet kernels.

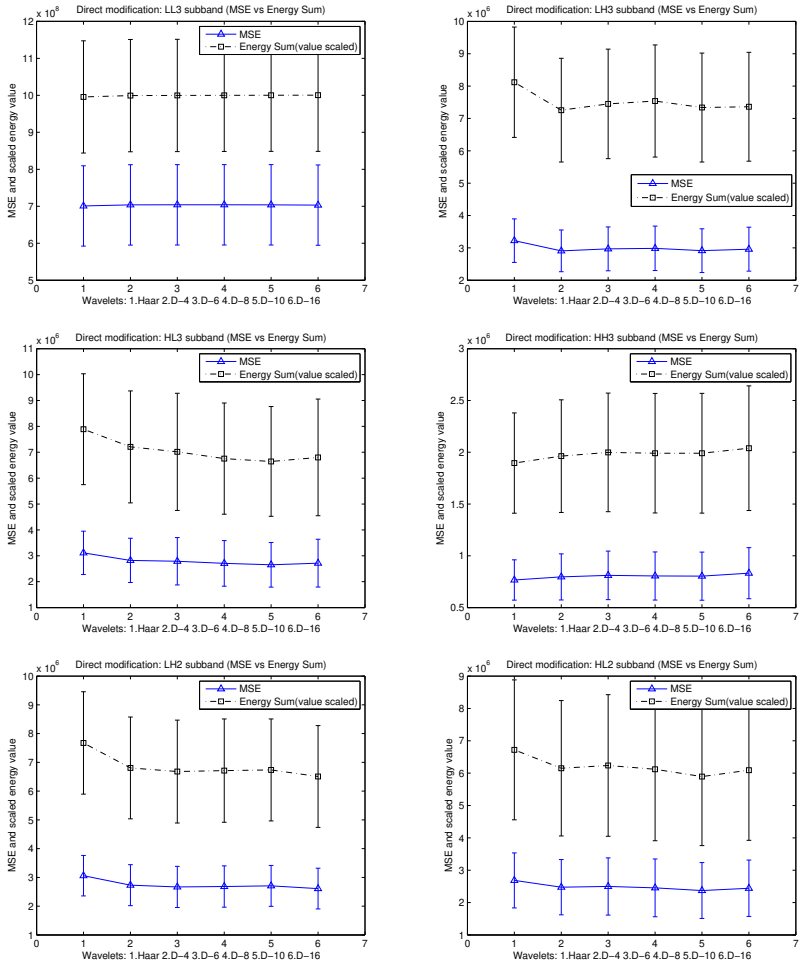

Fig. 4. Watermark embedding (Direct Modification) performance graph for different subbands. Six different wavelet kernels used here such as 1. Haar, 2. D-4, 3. D-6, 4. D-8, 5. D-10 and 6. D-16, respectively. Subbands are shown left to right and top to bottom: LL3, LH3, HL3, HH3, LH2 and HL2, respectively.

5 Conclusions

We have presented a generalised model for embedding distortion performance analysis of wavelet based watermarking schemes. With this mathematical analysis model we have achieved two different goals: generalisation of wavelet based embedding schemes and the effect of input parameters on distortion performance. We have proposed the model for orthonormal wavelet bases following the Parseval's Equality. Our model suggests that in a wavelet based watermarking scheme the MSE of the watermarked image is directly proportional to the sum of energy of the modification values of the selected wavelet coefficients. We have veri-

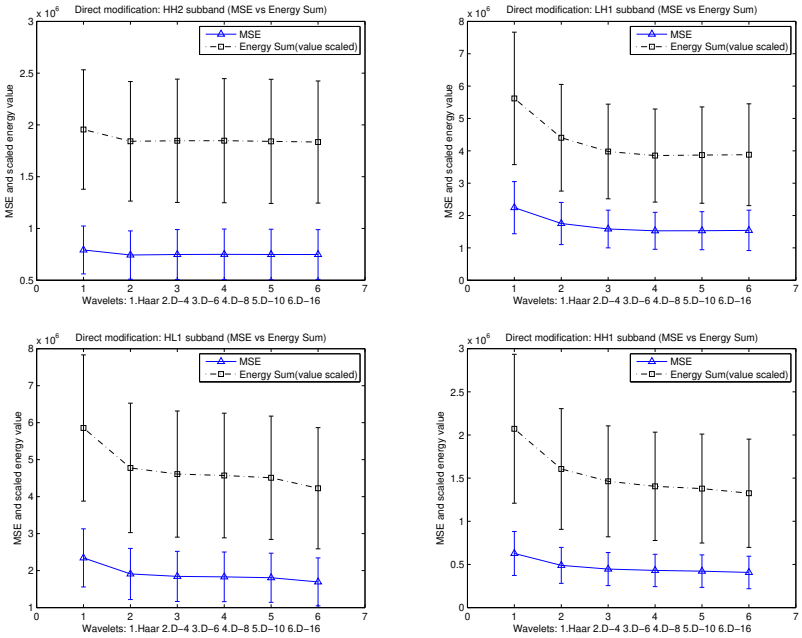

Fig. 5. Watermark embedding (Direct modification) performance graph for different subbands. Six different wavelet kernels used here such as 1. Haar, 2. D-4, 3. D-6, 4. D-8, 5. D-10 and 6. D-16, respectively. Subbands are shown left to right and top to bottom: HH2, LH1, HL1, HH1.

fied the model by evaluating the embedding distortion performance for different choices of wavelet kernels, subbands and the coefficient selections used in wavelet based watermark embedding. The experimental simulation successfully verified the proposed model.

Acknowledgments: This work is funded by BP-EPSRC Dorothy Hodgkin postgraduate award.

References

1. Xia, X., Boncelet, C.G., Arce, G.R.: Wavelet transform based watermark for digital images. Optic Express **3**(12) (Dec. 1998) 497–511
2. Kim, J.R., Moon, Y.S.: A robust wavelet-based digital watermarking using level-adaptive thresholding. In: Proc. IEEE ICIP. Volume 2. (1999) 226–230
3. Huo, F., Gao, X.: A wavelet based image watermarking scheme. In: Proc. IEEE ICIP. (Oct. 2006) 2573–2576
4. Kundur, D., Hatzinakos, D.: Digital watermarking using multiresolution wavelet decomposition. In: Proc. IEEE ICASSP. Volume 5., Seattle, WA, USA (May 1998) 2969–2972

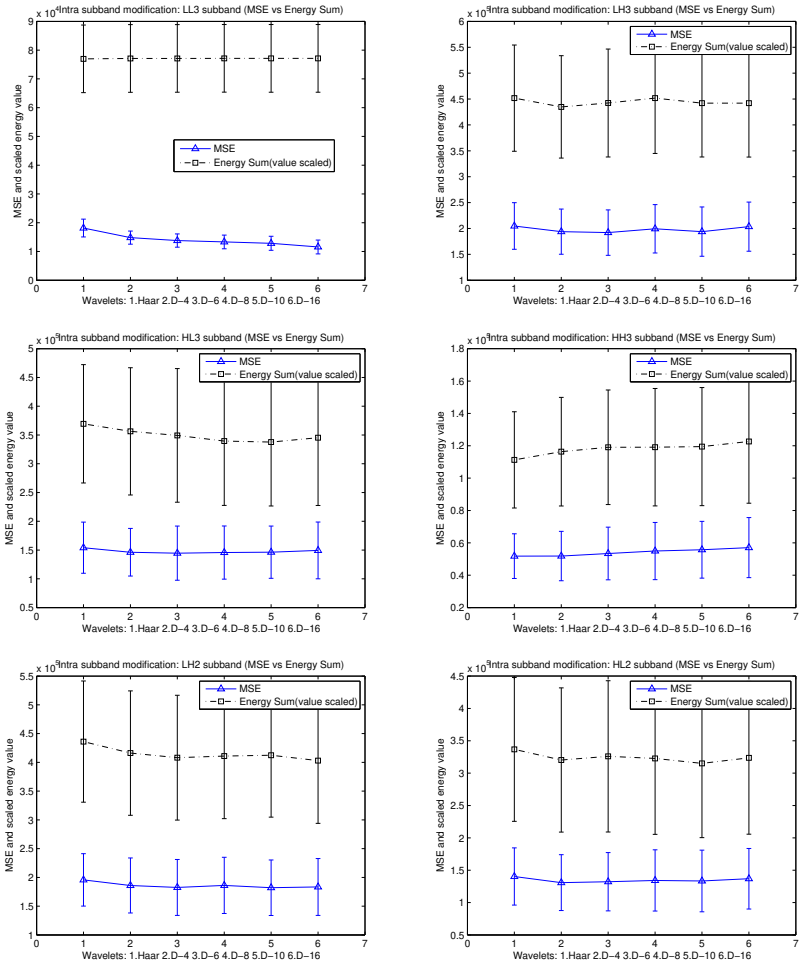

Fig. 6. Watermark embedding (Intra subband modification) performance graph for different subbands. Six different wavelet kernels used here such as 1. Haar, 2. D-4, 3. D-6, 4. D-8, 5. D-10 and 6. D-16, respectively. Subbands are shown left to right and top to bottom: LL3, LH3, HL3, HH3, LH2 and HL2, respectively.

5. Wang, H.J., Su, P.C., Kuo, C.C.J.: Wavelet-based digital image watermarking. Optics Express **3** (Dec. 1998) 491–497
6. Xie, L., Arce, G.R.: Joint wavelet compression and authentication watermarking. In: Proc. IEEE ICIP. Volume 2. (1998) 427–431
7. Barni, M., Bartolini, F., Piva, A.: Improved wavelet-based watermarking through pixel-wise masking. IEEE Trans. Image Processing **10**(5) (May 2001) 783–791
8. Jin, C., Peng, J.: A robust wavelet-based blind digital watermarking algorithm. Information Technology Journal **5**(2) (2006) 358–363
9. Gong, Q., Shen, H.: Toward blind logo watermarking in JPEG-compressed images. In: Proc. Int'l conf. on parallel and distributed computing, applications and

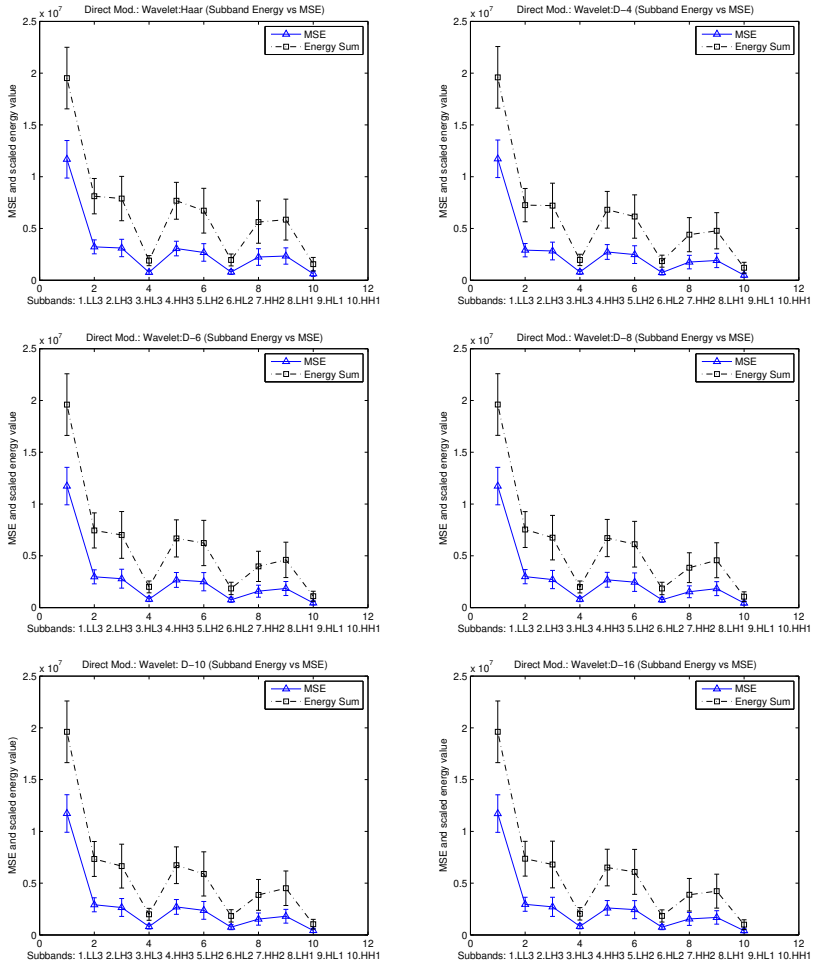

Fig. 7. Watermark embedding (Direct Modification) performance graph for various wavelets in different subband. Wavelet kernels are shown left to right and top to bottom: Haar, D-4, D-6, D-8, D-10 and D-16, respectively.

technologies (PDCAT 2005). (Dec. 2005) 1058–1062

10. Feng, X.C., Yang, Y.: A New Watermarking Method Based on DWT. Lecture Notes in Computer Science **3802** (2005) 1122–1126
11. Kundur, D., Hatzinakos, D.: Toward robust logo watermarking using multiresolution image fusion principles. IEEE Trans. Multimedia **6**(1) (Feb. 2004) 185–198
12. Ejima, M., Miyazaki, A.: On the evaluation of performance of digital watermarking in the frequency domain. In: Proc. IEEE ICIP. Volume 2. (Oct. 2001) 546–549
13. Bhowmik, D., Abhayaratne, C.: Evaluation of watermark robustness to JPEG2000 based content adaptation attacks. In: Proc. IET Int'l Conf. on Visual Info. Eng. (VIE '08). (Jul.-Aug. 2008) 789–794

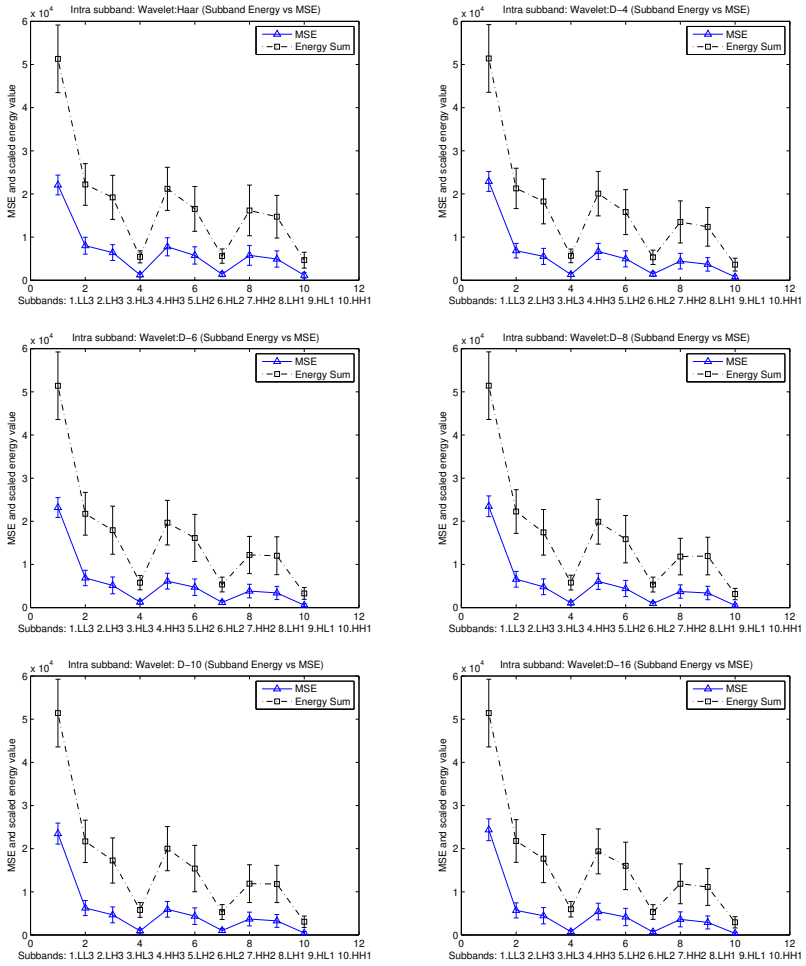

Fig. 8. Watermark embedding (Intra subband modification) performance graph for various wavelets in different subband. Wavelet kernels are shown left to right and top to bottom: Haar, D-4, D-6, D-8, D-10 and D-16, respectively.

14. Zhang, Z., Mo, Y.L.: Embedding strategy of image watermarking in wavelet transform domain. In: Proc. Image Compression and Encryption Technologies. Volume 4551., SPIE (2001) 127–131
15. Vetterli, M., Kovačevic, J.: Wavelets and subband coding. Prentice-Hall, Inc., Upper Saddle River, NJ, USA (1995)
16. Daubechies, I., Sweldens, W.: Factoring wavelet transforms into lifting steps. J. Fourier Anal. Appl. **4**(3) (1998) 245–267